

Article

Pressure Induced Disorder-Order Phase Transitions in the Al₄Cr Phases

Changzeng Fan ^{1,2,*}, Xu Geng ^{1,2} and Bin Wen ¹

¹ State Key Laboratory of Metastable Materials Science and Technology, Yanshan University, Qinhuangdao 066004, China; gengxuysl@126.com (X.G.); wenbin@ysu.edu.cn (B.W.)

² Hebei Key Lab for Optimizing Metal Product Technology and Performance, College of Materials Science and Technology, Yanshan University, Qinhuangdao 066004, China

* Correspondence: chzfan@ysu.edu.cn

Abstract: An ordered ω -Al₄Cr phase synthesized recently by a high-pressure sintering (HPS) approach was calculated to be stable by density function theory (DFT), implying that high pressure can accelerate the disorder-order phase transitions. The structural building units of the ω -Al₄Cr phase as well as the non-stoichiometric disordered ϵ -Al₄Cr and μ -Al₄Cr phases have been analyzed by the topological “nanocluster” method in order to explore the structural relations among these phases. Both the ϵ - and μ -Al₄Cr phases contain the typical Macky or pseudo-Macky cluster, and their centered positions were all occupied by Cr atoms, which all occupy the high-symmetry Wyckoff positions. The mechanism of the pressure-induced disorder-order phase transitions from the ϵ -/ μ -Al₄Cr to the ω -Al₄Cr phase has been analyzed, and the related peritectic and eutectoid reactions have been re-evaluated. All results suggest that the stable ω -Al₄Cr phase are transformed from the μ -Al₄Cr phase by the eutectoid reaction that is accelerated by high-pressure conditions, whereas the ϵ -Al₄Cr phase should form by the peritectic reaction.

Keywords: Al₄Cr; intermetallics; high-pressure; disorder-order; phase transitions



Citation: Fan, C.; Geng, X.; Wen, B.

Pressure Induced Disorder-Order Phase Transitions in the Al₄Cr Phases. *Crystals* **2022**, *12*, 1008. <https://doi.org/10.3390/cryst12071008>

Academic Editor: Daniel Errandonea

Received: 23 June 2022

Accepted: 19 July 2022

Published: 21 July 2022

Publisher’s Note: MDPI stays neutral with regard to jurisdictional claims in published maps and institutional affiliations.



Copyright: © 2022 by the authors. Licensee MDPI, Basel, Switzerland. This article is an open access article distributed under the terms and conditions of the Creative Commons Attribution (CC BY) license (<https://creativecommons.org/licenses/by/4.0/>).

All materials are disordered at a finite temperature and the high temperature provides significant entropic stabilization of phases relative to low-temperature ordered structures [1–4]. Although the influence of pressure on the solidification and phase transformation has not been studied as widely as that of temperature, investigations on the effects of pressure on the material’s thermodynamics has become popular recently [5–7]. For example, the pressure-induced fast ordering phase transition (disordered-fcc to ordered-fcc) structures in a CoCrCuFeNiPr high-entropy alloy was found at the pressure ranging from 7.8 GPa to 16.0 GPa [8]. More recently, a pressure-induced inverse order-disorder transition was reported in double perovskites, Y₂CoIrO₆ and Y₂CoRuO₆ [9]. There are also different options for computational methods for high-pressure phase transitions [10–13].

The Al-rich Al-Cr intermetallic phases, ϵ -Al₄Cr, μ -Al₄Cr and η -Al₁₁Cr₂, exhibit as prototypes of complex metallic alloys related to the formation of icosahedral quasicrystals (IQC). Historically, the ϵ -Al₄Cr phase has been wrongly considered as the η -Al₁₁Cr₂ phase by Audier et al. [14] and finally determined by Li et al. [15]. Furthermore, the ϵ -Al₄Cr phase has also been found to be structurally related to the icosahedral quasicrystal by Wen et al. [16]. Different from the orthorhombic ϵ -Al₄Cr phase, the μ -Al₄Cr phase has hexagonal symmetry that had been frequently observed [17], and its crystal structure was finally determined and found in close relation with the η -Al₁₁Cr₂ phase by Cao et al. [17,18]. However, the ϵ -Al₄Cr and μ -Al₄Cr phases are both non-stoichiometric disordered phases. Therefore, it is very interesting that an ordered ω -Al₄Cr phase has been discovered by the high-pressure sintering (HPS) approach recently in our group [19].

In the present work, DFT calculations have been carried out in order to explore the stability of the ordered ω -Al₄Cr phase. Then, the topological “nanocluster” method was

employed to study the structural relations among the ϵ -, μ - and ω -Al₄Cr phases. Finally, the thermodynamic analysis was performed to understand the mechanism of the pressure-induced disorder-order phase transitions.

All first-principles calculations were carried out with the DFT calculations method as implanted in the Vienna ab initio simulation package (VASP) [20]. The generalized gradient approximation (GGA) in the Perdew-Burke-Ernzerhof (PBE) form [21] was used to describe the exchange-correlation function, and the projected augmented wave (PAW) method [22] was used to describe the pseudopotentials, i.e., to deal with the core and valence electrons. The k-point samplings in the Brillouin zone were performed using the Monkhorst-Pack scheme [23]. A $5 \times 1 \times 5$ mesh k-point and a 500-eV plane-wave cutoff energy have been tested to satisfy the strict force gradient (EDIFFG) self-consistent convergence criterion: 1×10^{-6} eV/atom. From the calculation results shown in Figure 1, one can find that the ω -Al₄Cr phase is thermodynamically stable as its formation energy lies on the convhull along with other stable phases, such as AlCr₂ and Al₄₅Cr₇ (Al₃Cr becomes metastable) of the Al-Cr system from the open quantum materials database (OQMD) [24]. Such findings reveal that high pressure can accelerate the disorder-order phase transitions from the ϵ -/ μ -Al₄Cr to the ω -Al₄Cr phase. Therefore, it is necessary to understand the structural relations between these phases and to decipher the phase transition mechanisms.

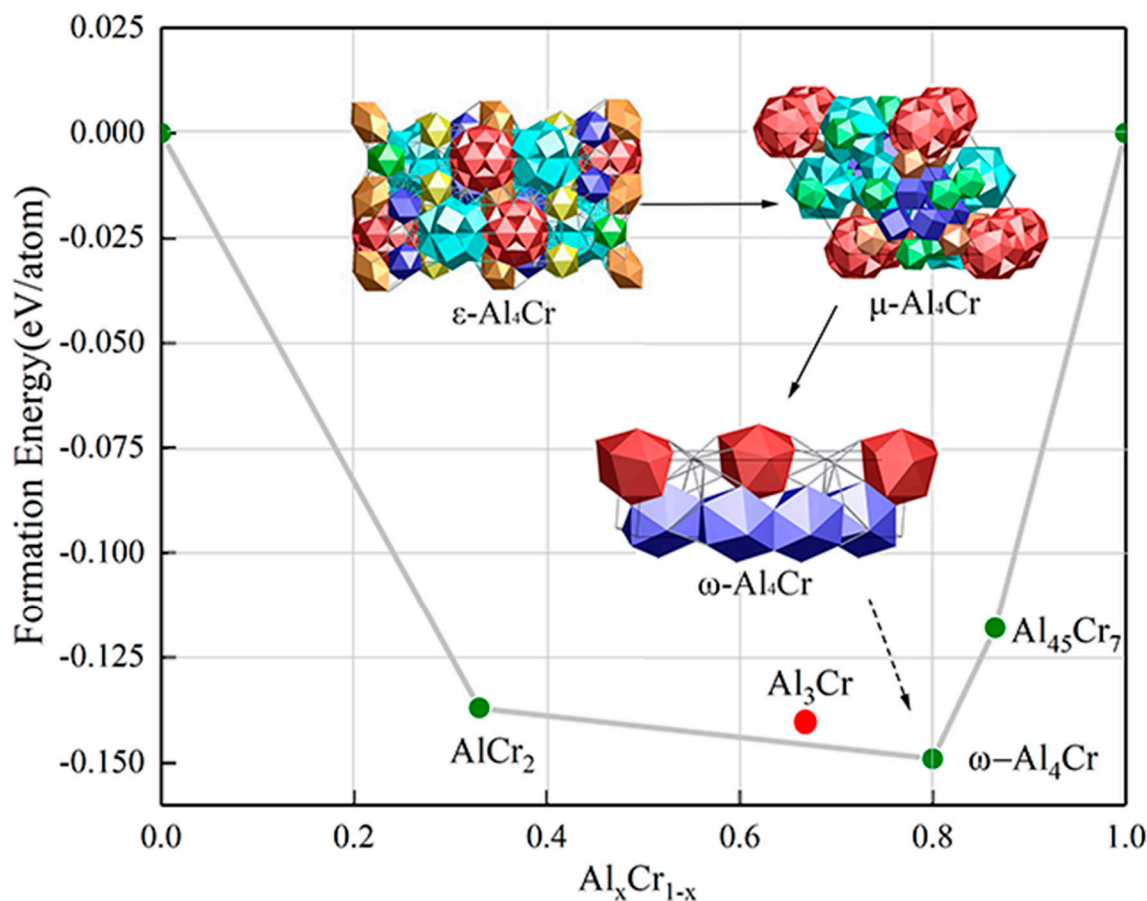


Figure 1. Convhull of the Al-Cr system by first-principles calculations with the proposed phase transition sequences for the ϵ -, μ - and ω -Al₄Cr phases in the present work.

The “nanocluster” method in the ToposPro package [25–28] was adopted to explore the topological features of the titled Al₁₁Cr₂ and its related crystal structures. The following criteria needs to be emphasized among all the algorithms used to determine the composition and structure of nanoclusters: (i) the clusters are represented as shell graphs with centers at the most symmetrical positions; (ii) the clusters do not interpenetrate and include all atoms

of the structure, making the “nanocluster” method ideal for exploring the building units of intermetallics, including the ϵ -Al₄Cr [26].

The ϵ -Al₄Cr phase is an extremely complex intermetallic compound with 682 atoms in the unit cell. We have re-analyzed the structural building units of the ϵ -Al₄Cr phase by the nanoclustering procedure in order to explore the similarities between the ϵ -Al₄Cr phase and the μ -Al₁₁Cr₂ phase, although it has been carried out previously and it captured the Mackay polyhedral [26] that was misled by Li et al. [15].

Figure 2 shows the nanocluster model of the ϵ -Al₄Cr phase which is composed of six clusters: Cr₁₀(2)(1@12@42), Al₁₃(2)(1@12@46), Cr₅(1)(1@12), Al₂₆(1)(1@10), Cr₉(1)(1@12) and Al₂(1)(1@12). Firstly, it is confirmed that Mackay clusters centered by Cr₁₀ atoms do exist and are similar to the double-shell cluster Cr₁₁(2)(1@12@38) (not shown here). Secondly, the ϵ -Al₄Cr also contains another double-shell cluster, which is Al₁₃(2)(1@12@46).

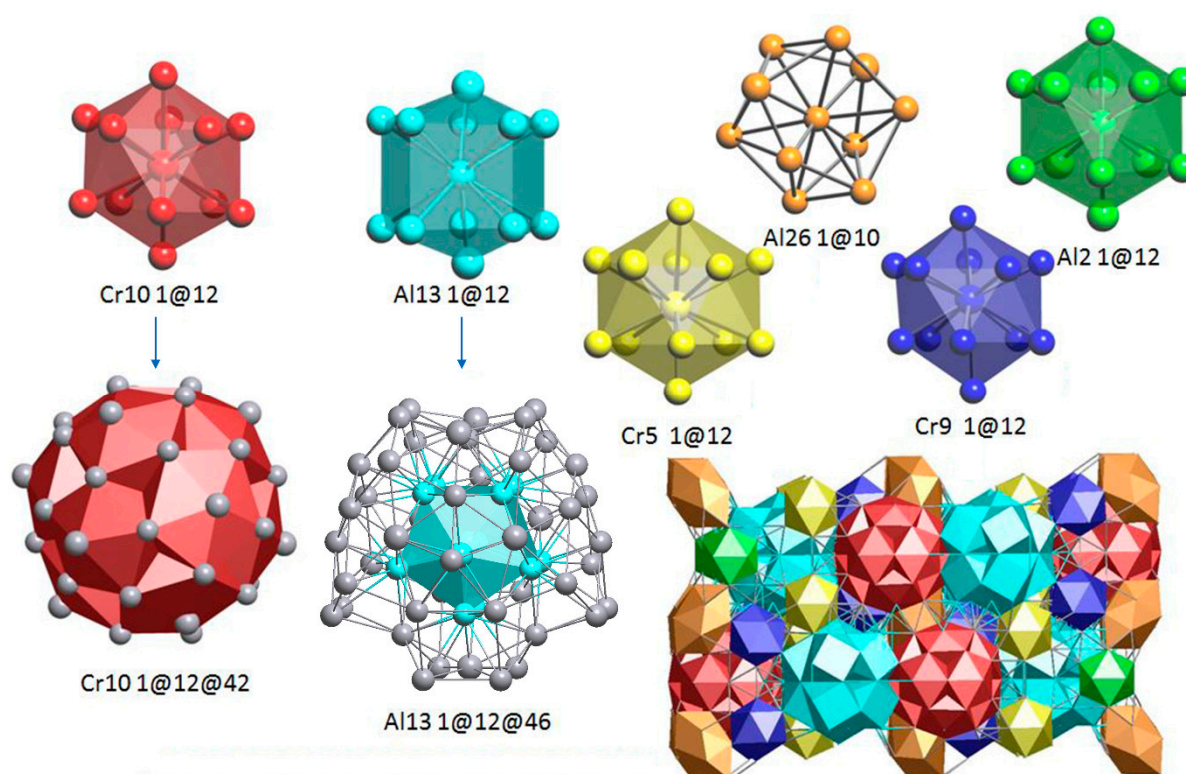


Figure 2. The entire unit cell of ϵ -Al₄Cr structure composed of six cluster units.

Figure 3 shows one kind of nanocluster model of the μ -Al₄Cr phase, which contains six clusters: Cr₂(2)(1@12@41), Al₂₂(2)(1@12@46), Al₂₄(1)(1@12), Cr₃(1)(1@12), Al₃₂(1)(1@12) and Al₃₁(0). The pseudo-Mackay polyhedral appears in the form of Cr₂(2)(1@12@41); the icosahedra first cell was replaced by an irregular 12-coordinated polyhedron although there are only 41 atoms instead of 42, owing to the line-shared instead of vertex-shared pentagonal curved planes. Interestingly, the double-shell clusters, Al₂₂(2)(1@12@46) appear again as Al₁₃(2)(1@12@46) in the ϵ -Al₄Cr. The rest of the clusters include one pentahedron and two icosahedrons, which are very popular in Al-Cr quasicrystal approximants besides one single-atom-type cluster.

To compare the ϵ - and μ -Al₄Cr phase, both phases contain a 1@12@42 Mackay or pseudo-Mackay cluster, which is known as one of the most viable structural units for complex metallic alloys and quasicrystals and their approximants. The centered positions inside the Mackay or pseudo-Mackay cluster were all occupied by Cr atoms and these Cr atoms all occupy the high-symmetry Wyckoff positions (See Table S1 in the Supplementary Materials). Very interestingly, the 1@12@46 double-shell nanocluster also appears in both

phases, as shown in Figure 4. Figure 4a,b represents the 1@12@46 nanoclusters found in ϵ -Al₄Cr and μ -Al₄Cr, and the marked four red balls are the Cr atoms and the four yellow balls are the Al atoms. For the ω -Al₄Cr phase, the building unit cluster is quite simple as it contains only 30 rather than several hundred atoms. There are two types of distinct coordination polyhedrals around two chromium atoms in the ω -Al₄Cr phase; the first one connects to eleven aluminum atoms whereas the second one is connected to ten aluminum atoms [19], implying it has a completely different configuration with those of the ϵ - and μ -Al₄Cr phase.

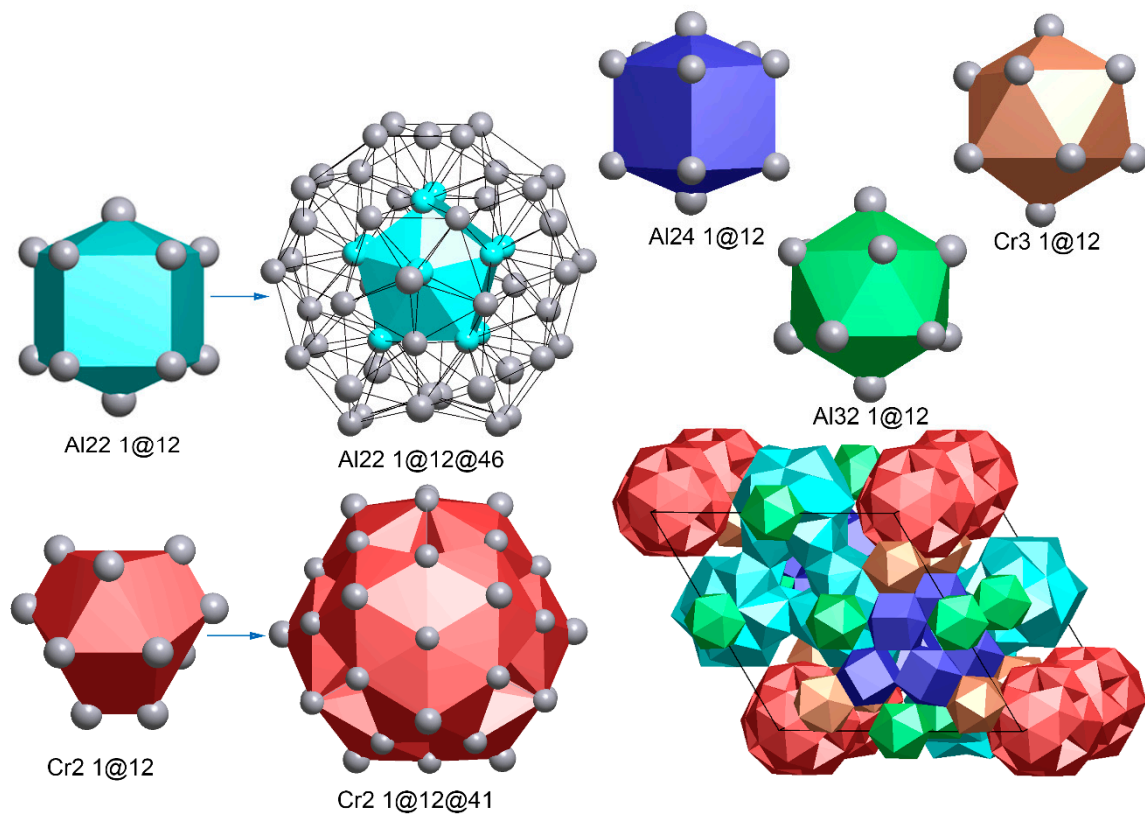


Figure 3. The entire unit cell of μ -Al₄Cr structure composed of six cluster units.

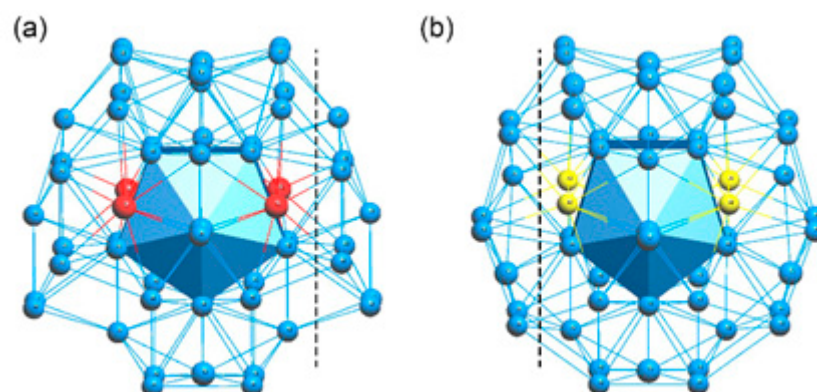


Figure 4. The 1@12@46 nanoclusters found in (a) ϵ -Al₄Cr and (b) μ -Al₄Cr.

Concerning the large unit cell of all these titled complex metallic alloys, density-functional-theory (DFT)-based methods are not plausible as a huge computational cost is required. As a novel tool for the efficient prediction of a material's properties, machine learning has emerged, and it claims that the machine-learned models for the formation energy of compounds can approach the accuracy of DFT. In the present work, we choose

the deep neural network model named ElemNet [29] to estimate the formation energies and the molar fragment descriptor (MFD) [30] to predict the vibrational free energies and entropies, along with the property-labeled material fragments (PLMF) methods [31] to predict the bulk and shear moduli.

Conventional machine learning approaches for predicting a material's properties involves representing the material composition in the model input format, manual feature engineering, and selection by incorporating the necessary domain knowledge and human intuition by computing the very important chemical and physical attributes of each element, and finally to construct the predictive model. However, "ElemNet" is a deep neural network model which can bypass conventional, manual feature engineering requiring domain knowledge, and it automatically captures the physical and chemical interactions and similarities between different elements to predict the material's properties, such as the formation enthalpy, with better accuracy and speed. The "ElemNet" model have been trained on the DFT-computed formation enthalpies of 275, 759 compounds with unique elemental compositions from the Open Quantum Materials Database (OQMD) [29].

The calculation of stability at high temperatures is fundamental for the prediction of phase diagrams and chemical reactions. Solving this problem is challenging as high-throughput (HT) phase diagrams have typically been calculated using the ab initio formation enthalpies at 0 K. Legrain et al. show that several machine learning approaches can be applied to the calculation of vibrational entropies and free energies (Svib and Fvib) of solids with satisfactory accuracy and reasonable computational expense. Practically, they have tested a set of descriptors simply based on the chemical formula of compounds and by training a set of 25,705 compounds in the Inorganic Crystal Structure Database (ICSD). They concluded that the descriptors based on the chemical composition and the elemental properties of atoms of the material perform best for small training sets [30].

Bulk/shear moduli are both predicted within the property-labeled material fragments (PLMF) scheme. In this approach, data from the ab initio calculated AFLOW repository is combined with the quantitative material's structure–property relationship models. The prediction only requires the structural information and has comparable accuracy with those of the training data (2829 materials were extracted from the AFLOW repository) [31].

The calculated results of the above mentioned five phases are shown in Table 1. For the ElemNet and the MFD methods, only chemical compositions are necessary, whereas for the PMLF method, the configurations of phases are required. In the present work, the stoichiometric compositions of both the ordered and disordered phases have been calculated and listed, but only the properties of ordered phases are considered and compared. From the calculated stoichiometric values in Table 1, one can find that all disordered phases of ϵ -Al₄Cr and μ -Al₄Cr are deficient of Al element compared to the corresponding ordered phases. Such universal deficiency of Al atoms could be understood from the close-packed FCC Al compared to the non-close-packed BCC Cr. The calculated vibrational free energy and entropy of Cr (−3.24 meV/atom) compared to Al (15.29 meV/atom) by the MFD method also suggests that the Cr atoms diffuse more easily than Al atoms. It is found that the bulk modulus values of different Al–Cr alloys are between 105 and 122 GPa; these values are close to the average between the bulk modulus of Cr (182–185 GPa) [32] and Al (73 GPa) [33]. Strikingly, not only stoichiometric, but all the predicted properties including formation energies, vibrational free energies and entropies, and bulk modulus and shear modulus of the ordered phases of ϵ -Al₄Cr and μ -Al₄Cr are nearly equivalent (see Table 1). Although, both phases have completely different crystallographic symmetry and have quite different stoichiometric disordered structural models. Such findings encourage us to deduce that the forming conditions of both phases are indistinguishable, and the ϵ -Al₄Cr should also be the precursor in the forming of the η -Al₁₁Cr₂ phase by the peritectic reaction as that of μ -Al₄Cr phase [34]:

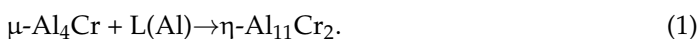


Table 1. Formation Energy (eV/atom), vibrational free energy and entropy, bulk modulus and shear modulus of related phases in the Al-Cr system by the deep neural network model.

Phases	Stoichio-Metric	Al:Cr Ratio	E_f^a	$F_{\text{vib}}/S_{\text{vib}}^b$	B (GPa) ^c	G (GPa) ^c
ϵ -Al ₄ Cr	472:112 (449.1:114.3)	4.21 (3.93)	−0.167	12.43	110.70	79.18
μ -Al ₄ Cr	464:110 (457.6:110)	4.22 (4.16)	−0.167	12.43	106.01	76.97
η -Al ₁₁ Cr ₂	516:100 (516:100)	5.16 (5.16)	−0.15	12.90	105.77	62.76
ω -Al ₄ Cr	24:6	4.0	−0.167	12.29	121.65	81.56
θ -Al ₄₅ Cr ₇	90:14	6.43	−0.13	13.34	109.23	56.82

^a Reference [29]; ^b Reference [30]; ^c Reference [31]. For the method introduced in Reference [20], the calculations were carried out on the website: <http://info.eecs.northwestern.edu/FEpredictor> (only the stoichiometric of compounds is required as input, accessed on 13 July 2022). For the method introduced in References [30,31], the calculations were carried out on the website: <https://aflo.org/aflo-ml/>, (only the structural information in the VASP format is required as input, accessed on 13 July 2022).

The structural building units of the ϵ -Al₄Cr and μ -Al₄Cr discussed before also support that they are nearly indistinguishable as both phases have identical or slightly different clusters. It was also mentioned that the following eutectoid reaction has been observed: η -Al₁₁Cr₂ → μ -Al₄Cr + θ -Al₇Cr (Al₄₅Cr₇) [34]. It needs to be noted that the situation should be more complicated as both the η -Al₁₁Cr₂ and μ -Al₄Cr phase are non-stoichiometric compounds (see Table 1). The Al:Cr ratio equals to 5.16 in the η -Al₁₁Cr₂ phase. The Al:Cr ratio equals to 4.2 for both the ϵ -Al₄Cr and μ -Al₄Cr phase, and the only exception is the ω -Al₄Cr whose Al:Cr ratio is exactly equal to 4. In addition, the stable ω -Al₄Cr should be the final product of the eutectoid reaction as it has the lowest formation energy (see Figure 1).

In the present work, high pressure affects the solidification in synergy with high temperature, which makes the situation more complex. It is essential to explain the pressure-induced disorder-order phase transitions (disordered ϵ -Al₄Cr or/and μ -Al₄Cr to the ordered ω -Al₄Cr) firstly. The well-known thermodynamic potential difference between ordered and disordered phases at certain temperature T and pressure P is [4]:

$$\Delta G \equiv G_{\text{dis}} - G_{\text{ord}} = \Delta E - T\Delta S + P\Delta V \quad (2)$$

where ΔG means the thermodynamic potential difference between that of disordered phase G_{dis} and ordered phase G_{ord} ; ΔE and ΔS are the internal energy and entropy difference between the ordered and disordered phases. If $\Delta G > 0$, then the ordered phase is favorable. For simplicity, we take the disordered μ -Al₄Cr to compare with the ordered ω -Al₄Cr phase as there are only two vacancy positions in the former phase. As the first term $\Delta E > 0$ is generally satisfied owing to the local distortion, it will enhance the internal energy of the disordered phase. Therefore, $\Delta G > 0$ will be satisfied even when the sum of the second and third terms equal to zero. Taking the HPS conditions, 5GPa and 1169 K, into consideration, the second term and the third term equals to −3.4 eV and 7.3 eV, respectively. Therefore, $\Delta G > 0$ is satisfied at HPS conditions in synthesizing the ω -Al₄Cr phase, and the ordered ω -Al₄Cr phase is more stable than the disordered μ -Al₄Cr phase. It can also expect that the critical pressure to ignite the disorder to order phase transition is about 2.3 GPa from the same thermodynamic potential difference calculations. Comparing the ϵ -Al₄Cr and μ -Al₄Cr, it is obvious that the former is more disordered as it contains more vacancy positions (7 vs. 2), besides the additional ten co-occupied positions, than the latter. The increasing of entropy caused by the vacancy positions was calculated to be about $118k_B$, which corresponds to 10.8 eV at 1058 K (the eutectoid reaction temperature). If there exists a phase transition from the ϵ -Al₄Cr to the μ -Al₄Cr phase directly, the external pressure required should be around 22.5 GPa. In other words, high pressure (5 GPa) will probably affect the solidification by reducing the diffusion coefficients of the involved atoms, but it has little effect on a possible phase transition from the ϵ -Al₄Cr to the μ -Al₄Cr phase.

In the following, the peritectic and eutectoid reactions based on the above discussions are reconsidered. It is most likely that the ϵ -Al₄Cr phase appears firstly by the peritectic reaction, and then the μ -Al₄Cr phase was produced by the eutectoid reaction: (1) there are more disordered atoms in the ϵ -Al₄Cr and the η -Al₁₁Cr₂ phases than that of the μ -Al₄Cr phase which has only two vacancy positions, thus the formation energies of the ϵ -Al₄Cr and the η -Al₁₁Cr₂ phases should be much closer; (2) the solidification is controlled by the diffusion of the involved atoms, especially the sluggish Al atoms, thus the Al-deficiency ϵ -Al₄Cr phase (the Al:Cr ratio 3.93 and 4.16 for the disordered ϵ -Al₄Cr and the μ -Al₄Cr phase, respectively) should be formed firstly; (3) the transformation from the μ -Al₄Cr phase to the ω -Al₄Cr phase is easily understood from the pressure-induced disorder-order transition mechanism.

In summary, the mechanism of the pressure-induced disorder-order phase transitions in the Al₄Cr system have been analyzed. The thermodynamic analysis results suggest that the stable ω -Al₄Cr phase is transformed from the μ -Al₄Cr phase by the eutectoid reaction accelerated by high-pressure conditions. The ϵ -Al₄Cr phase should form by the peritectic reaction, although its structural building units are nearly indistinguishable from that of the μ -Al₄Cr phase. The modified reaction process can also be understood easily by the diffusion-controlled solidification and phase transition. Such findings could be utilized to tune the final products with different phases and different mechanical properties on the one hand, and on the other hand would promote the understanding of the process of solidification including the forming mechanism of the quasicrystal phases in the Al-Cr binary system.

Supplementary Materials: The following are available online at <https://www.mdpi.com/article/10.3390/cryst12071008/s1>, Table S1: The Wyckoff positions of the centered atoms inside the Macky or pseudo-Macky cluster for the ϵ - and μ -Al₄Cr phase along with the η -Al₁₁Cr₂ phase

Author Contributions: Conceptualization, C.F.; investigation, X.G. and C.F.; writing—original draft preparation, C.F. and X.G.; writing—review and editing, X.G., C.F. and B.W.; project administration, C.F.; funding acquisition, C.F. and B.W. All authors have read and agreed to the published version of the manuscript.

Funding: This work was supported by: The National Natural Science Foundation of China (grant No. 52173231/51771165), the Natural Science Foundation of Hebei Province (grant No. E2022203182) and Hebei Province Innovation Ability Promotion Project (22567609H).

Institutional Review Board Statement: Not applicable.

Informed Consent Statement: Not applicable.

Data Availability Statement: Not applicable.

Conflicts of Interest: The authors declare no conflict of interest.

References

1. Simonov, A.; Goodwin, A.L. Designing disorder into crystalline materials. *Nat. Rev. Chem.* **2020**, *4*, 657–673. [[CrossRef](#)]
2. Redfem, S.A.T. Order-Disorder Phase Transitions. *Rev. Miner. Geochem.* **2000**, *39*, 105–133.
3. Skakunova, K.D.; Rychkov, D.A. Low Temperature and High-Pressure Study of Bending L-Leucinium Hydrogen Maleate Crystals. *Crystals* **2021**, *11*, 1575. [[CrossRef](#)]
4. Errandonea, D. Pressure-Induced Phase Transformations. *Crystals* **2020**, *10*, 595. [[CrossRef](#)]
5. Baty, S.; Burakovsky, L.; Errandonea, D. *Ab Initio* Phase Diagram of Copper. *Crystals* **2021**, *11*, 537. [[CrossRef](#)]
6. Anzellini, S.; Burakovsky, L.; Turnbull, R.; Bandiello, E.; Errandonea, D. P–V–T Equation of State of Iridium Up to 80 GPa and 3100 K. *Crystals* **2021**, *11*, 452. [[CrossRef](#)]
7. Baty, S.; Burakovsky, L.; Preston, D. Topological Equivalence of the Phase Diagrams of Molybdenum and Tungsten. *Crystals* **2020**, *10*, 20. [[CrossRef](#)]
8. Ma, Y.; Fan, J.; Zhang, L.; Zhang, M.; Cui, P.; Dong, W.; Yu, P.; Li, Y.; Liaw, P.K.; Li, G. Pressure-induced ordering phase transition in high-entropy alloy. *Intermetallics* **2018**, *103*, 63–66. [[CrossRef](#)]
9. Deng, Z.; Kang, C.J.; Croft, M.; Li, W.M.; Shen, X.; Zhao, J.F.; Yu, R.C.; Jin, C.Q.; Kotliar, G.; Liu, S.Z.; et al. A Pressure-Induced Inverse Order–Disorder Transition in Double Perovskites. *Angew. Chem.* **2020**, *132*, 2–9.

10. Fedorov, A.Y.; Rychkov, D.A. Comparison of different computational approaches for unveiling the high-pressure behavior of organic crystals at molecular level. Case study of tolazamide polymorphs. *J. Struct. Chem.* **2020**, *61*, 1356–1366. [[CrossRef](#)]
11. Colmenero, F. Organic acids under pressure: Elastic properties, negative mechanical phenomena and pressure induced phase transitions in the lactic, maleic, succinic and citric acids. *Mater. Adv.* **2020**, *1*, 1399–1426. [[CrossRef](#)]
12. Korabel'nikov, D.V.; Zhuravlev, Y.N. Semi-empirical and ab initio calculations for crystals under pressure at fixed temperatures: The case of guanidinium perchlorate. *RSC Adv.* **2020**, *10*, 42204–42211. [[CrossRef](#)] [[PubMed](#)]
13. Rychkov, D.A. A Short Review of Current Computational Concepts for High-Pressure Phase Transition Studies in Molecular Crystals. *Crystals* **2020**, *10*, 81. [[CrossRef](#)]
14. Audier, M.; Durand-Charre, M.; Laclau, E.; Klein, H. Phase equilibria in the Al-Cr system. *J. Alloys Compd.* **1995**, *220*, 225–230. [[CrossRef](#)]
15. Li, X.Z.; Sugiyama, K.; Hiraga, K.; Sato, A.; Yamamoto, A.; Sui, H.X.; Kuo, K.H. Crystal structure of orthorhombic ϵ -Al₄Cr. *Zeitschrift Für Krist. Cryst. Mater.* **1997**, *212*, 628–633. [[CrossRef](#)]
16. Wen, K.Y.; Chen, Y.L.; Kuo, K.H. Crystallographic Al₄Cr Crystalline Relationships of the and Quasicrystalline Phases. *Metall. Trans. a-Phys. Metall. Mater. Sci.* **1992**, *23*, 2437–2445. [[CrossRef](#)]
17. Cao, B.; Kuo, K. Crystal structure of the monoclinic η -Al₁₁Cr₂. *J. Alloys Compd.* **2008**, *458*, 238–247. [[CrossRef](#)]
18. Cao, B. On the structure of the hexagonal μ -Al₄Cr and its relation to the monoclinic η -Al₁₁Cr₂. *J. Alloys Compd.* **2017**, *698*, 605–610. [[CrossRef](#)]
19. Fan, C.Z.; Liu, C. Crystal structure of ω -Al₄Cr. *IUCrData* **2018**, *3*, x180216. [[CrossRef](#)]
20. Kresse, G.; Furthmüller, J. Efficient iterative schemes for ab initio total-energy calculations using a plane-wave basis set. *Phys. Rev. B (Condens. Matter)* **1996**, *54*, 11169–11181. [[CrossRef](#)]
21. Perdew, J.P.; Burke, K.; Ernzerhof, M. Generalized gradient approximation made simple. *Phys. Rev. Lett.* **1996**, *77*, 3865. [[CrossRef](#)] [[PubMed](#)]
22. Blöchl, P.E. Projector augmented-wave method. *Phys. Rev. B Condens. Matter Mater. Phys.* **1994**, *50*, 17953–17979. [[CrossRef](#)] [[PubMed](#)]
23. Monkhorst, H.J.; Pack, J.D. Special points for Brillouin-zone integrations. *Phys. Rev. B* **1976**, *13*, 5188. [[CrossRef](#)]
24. Kirklin, S.; Saal, J.E.; Meredig, B.; Thompson, A.; Doak, J.W.; Aykol, M.; Rühl, S.; Wolverton, C.M. The Open Quantum Materials Database (OQMD): Assessing the accuracy of DFT formation energies. *NPJ Comput. Mater.* **2015**, *1*, 15010. [[CrossRef](#)]
25. Pankova, A.A.; Blatov, V.A.; Ilyushin, G.D.; Proserpio, D.M. Ilyushin, γ -Brass polyhedral core in intermetallics: The nanocluster model. *Inorg. Chem.* **2013**, *52*, 13094–13107. [[CrossRef](#)]
26. Akhmetshina, T.; Blatov, V.A. A fascinating building unit: Mackay cluster in intermetallics. *Struct. Chem.* **2016**, *28*, 133–140. [[CrossRef](#)]
27. Akhmetshina, T.G.; Blatov, V.A. Topological methods for complex intermetallics. *Zeitschrift für Kristallographie—Cryst. Mater.* **2017**, *232*, 497–506. [[CrossRef](#)]
28. Akhmetshina, T.G.; Blatov, V.A.; Proserpio, D.M.; Shevchenko, A.P. Topology of intermetallic structures: From statistics to rational design. *Acc. Chem. Res.* **2018**, *51*, 21–30. [[CrossRef](#)]
29. Jha, D.; Ward, L.; Paul, A.; Liao, W.K.; Choudhary, A.; Wolverton, C.; Agrawal, A. ElemNet: Deep Learning the Chemistry of Materials From Only Elemental Composition. *Sci. Rep.* **2018**, *8*, 17593. [[CrossRef](#)]
30. Legrain, F.; Carrete, J.; van Roekeghem, A.; Curtarolo, S.; Mingo, N. How Chemical Composition Alone Can Predict Vibrational Free Energies and Entropies of Solids. *Chem. Mater.* **2017**, *29*, 6220–6227. [[CrossRef](#)]
31. Isayev, O.; Oses, C.; Toher, C.; Gossett, E.; Curtarolo, S.; Tropsha, A. Universal fragment descriptors for predicting properties of inorganic crystals. *Nat. Commun.* **2017**, *8*, 15679. [[CrossRef](#)] [[PubMed](#)]
32. Anzellini, S.; Errandonea, D.; Burakovsky, L.; Proctor, J.E.; Turnbull, R.; Beavers, C.M. Characterization of the high-pressure and high-temperature phase diagram and equation of state of chromium. *Sci. Rep.* **2022**, *12*, 6727. [[CrossRef](#)] [[PubMed](#)]
33. Dewaele, A.; Loubeyre, P.; Mezouar, M. Equations of state of six metals above 94GPa. *Phys. Rev. B* **2004**, *70*, 094112. [[CrossRef](#)]
34. Cao, B.B. Structures of Quasicrystal Approximants in Al-Cr Alloys. Ph.D. Thesis, Dalian University Technology, Dalian, China, 2007. (In Chinese)